Biochimica et Biophysica Acta 1803 (2010) 1376–1385

Contents lists available at ScienceDirect

Biochimica et Biophysica Acta

journal homepage: www.elsevier.com/locate/bbamcr

Oxidative stress and alterations in actin cytoskeleton trigger glutathione efflux in *Saccharomyces cerevisiae*

Silvia Bradamante [a,*], Alessandro Villa [a], Silvia Versari [a], Livia Barenghi [b], Ivan Orlandi [c], Marina Vai [c]

[a] CNR-ISTM Institute of Molecular Science and Technologies, National Council of Research, via Golgi 19, 20133 Milan, Italy
[b] Visiting scientist at CNR-ISTM, Milan, Italy
[c] Department of Biotechnology and Biosciences, University of Milano-Bicocca, Piazza della Scienza 2, 20126 Milan, Italy

ARTICLE INFO

Article history:
Received 4 May 2010
Received in revised form 16 July 2010
Accepted 26 July 2010
Available online 12 August 2010

Keywords:
GSH
Oxidation
Actin
Yeast
Chloride channels
Microgravity

ABSTRACT

A marked deficiency in glutathione (GSH), the most abundant antioxidant in living systems, plays a major role in aging and the pathogenesis of diseases ranging from neurological disorders to early atherosclerosis and the impairment of various immunological functions. In an attempt to shed light on GSH homeostasis, we carried out the space experiment SCORE (*Saccharomyces cerevisiae* oxidative stress response evaluation) during the FOTON-M3 mission. Microgravity and hyperoxic conditions induced an enormous extracellular release of GSH from *S. cerevisiae* cells (≈40% w/dw), changed the distribution of the buds, and activated the high osmolarity glycerol (HOG) and cell integrity/PKC pathways, as well as protein carbonylation. The results from the single spaceflight experiment were validated by a complete set of experiments under conditions of simulated microgravity and indicate that cytoskeletal alterations are mainly responsible for the observed effects. The results of ground experiments in which we induced cytoskeletal modifications by means of treatment with dihydrocytochalasin B (DHCB), a potent inhibitor of actin polymerisation, or (*R*)-(+)-*trans*-4-(1-aminoethyl)-*N*-(4-pyridyl)cyclohexanecarboxamide dihydrochloride monohydrate (Y-27632), a selective ROCK (Rho-associated coiled-coil forming protein serine/threonine kinase) inhibitor, confirmed the role of actin in GSH efflux. We also found that the GSH release can be inhibited using the potent chloride channel blocker 5-nitro-2-(3-phenylpropylamino) benzoic acid (NPPB).

1. Introduction

Exposure to a spaceflight environment can induce multiple changes in living systems, such as increased stress hormone levels, insulin resistance, an altered immune response, and abnormal musculoskeletal system structure and function, which can have undesirable effects on normal physiological processes. Many of these effects parallel the alterations implicated in diseases of aging, but they occur and develop much more rapidly in space [1–3]. In particular, the space environment is associated with increased oxidative damage, which is possibly due to the generation of high-energy free radicals from radiation or changes in oxygen/intermediary metabolism. Russian investigators have found evidence indicating increased lipid peroxidation in human erythrocyte membranes after a long spaceflight and a decrease in some blood antioxidants [4]. It is well known that, to prevent oxidative damage, cells have developed a "multiple ways oxidative stress response" to counteract the effects of reactive oxygen species (ROS) by means of detoxifying enzymes (catalase, superoxide dismutase, and peroxidase) and thiol systems such as glutathione (GSH) and thioredoxin [5]. The livers of rats placed aboard Space Shuttle STS-63 for 8 days showed significantly decreased catalase, GSH reductase and GSH sulfur-transferase activities and dramatically decreased total liver GSH levels [6]. GSH plays a major role in a large number of cellular processes, such as differentiation, proliferation, and apoptosis, and alterations in GSH homeostasis are implicated in the development of a large number of human diseases ranging from cancer to cystic fibrosis, neurodegenerative disorders, and aging-related pathologies [7].

We have previously performed *in vitro* experiments under conditions of simulated microgravity (sim-μg) [8] and observed that *S. cerevisiae* exposed to oxidative stress releases significant amounts of endogenous GSH in the culture medium [9]. We chose yeast as our model system [10] because it is an ideal organism for studying the effects of oxidative damage [11,12]. It shares many antioxidant factors

Abbreviations: GSH, glutathione; SCORE, *Saccharomyces cerevisiae* oxidative stress response evaluation; DHCB, dihydrocytochalasin B; Y-27632, (*R*)-(+)-*trans*-4-(1-aminoethyl)-*N*-(4-pyridyl)cyclohexanecarboxamide dihydrochloride monohydrate; ROCK, Rho-associated coiled-coil forming protein serine/threonine kinase; NPPB, 5-nitro-2-(3-phenylpropylamino) benzoic acid; sim-μg, simulated microgravity; ROS, reactive oxygen species; GSH ER, glutathione extracellular release; CM, culture medium; CC, cell culture; VVM, variable volume module; EH, experiment hardware; RWV, rotating wall vessel; HARV, high aspect ratio vessel; HOG, high-osmolarity glycerol; PKC, protein kinase C; CFUs, colony-forming units; 1 *g*, gravity on ground; N, normoxia; H, hyperoxia

* Corresponding author.
E-mail address: silvia.bradamante@istm.cnr.it (S. Bradamante).

0167-4889/$ – see front matter © 2010 Elsevier B.V. All rights reserved.
doi:10.1016/j.bbamcr.2010.07.007

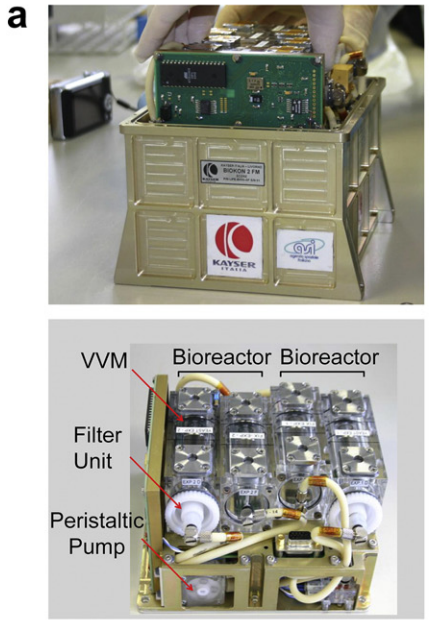

START: From t = L-7d (seven days before the FOTON-M3 launch) to t = L+7d, the *Saccharomyces cerevisiae* (0.25% DW in water) and the SM were in one VVM, while the other was filled up with fixatives.

STEP 1: At t = L+7d, SM was injected in the CC chamber to start the experiment.

STEP 2: At t = L+8d (24 hrs later), the yeast cells and SM were separated by filtration to end the experiment.

STEP 3: From t = L+8d to L+17d, the cells were preserved using a suitable fixative (Trichloroacetic acid 20%). Dithiothreitol was added to the medium to prevent GSH oxidation and protease and phosphatase inhibitors to prevent GSH degradation.

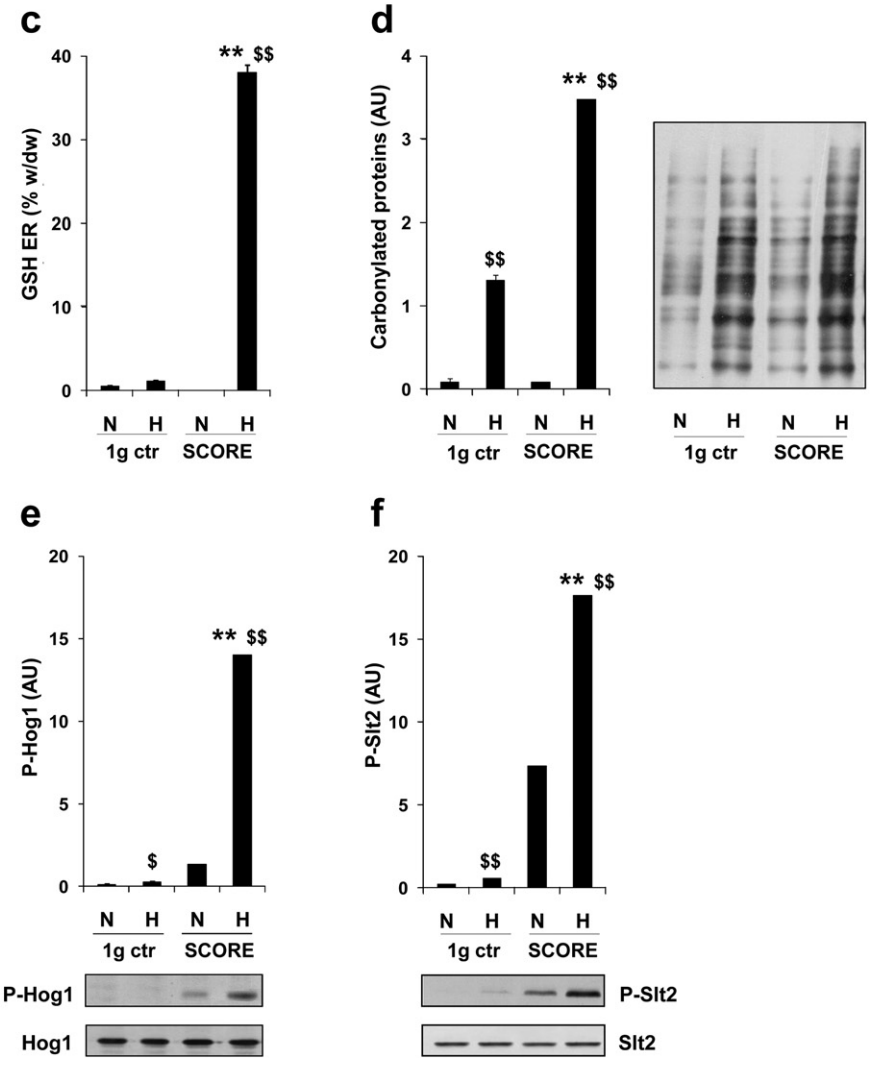

with mammalian cells but is much less demanding, which makes it perfect for both ground and space experiments in which the possibilities of temperature control and nutrient supplementation are limited. We selected an essential medium suitable for keeping the cells in a nondividing but metabolically active state and optimised for GSH production. Avoiding the use of free radical-generating compounds [13], we chose molecular oxygen as the oxidant because of the restrictions imposed by our spaceflight experimental setup and the reported evidence of hyperoxic damage [14]. In addition, the role of sim-μg in regulating *S. cerevisiae* gene expression and physiology has been extensively studied [15–17].

We participated in the 24-day FOTON-M3 space mission with the experiment SCORE (*Saccharomyces cerevisiae* oxidative stress response evaluation) to investigate the oxidative stress response of *S. cerevisiae* (particularly any alterations in GSH homeostasis) under conditions of real microgravity. Our hypothesis was that the consequences of a stress such as that induced by microgravity is the driving force behind the extracellular release of GSH (GSH ER). We here describe our spaceflight findings with ground controls (1*g* ctr) and supporting data obtained from sim-μg and 1 *g* experiments.

2. Materials and methods

2.1. Strain and culture conditions

S. cerevisiae L5267 (Lesaffre private strain collection, 0.25% dw) was incubated at 28 °C in 100 mL of culture medium (CM): KH_2PO_4 0.035 g, KOH 0.0037 g, $(NH_4)_2SO_4$ 0.07 g, $MgSO_4$ 0.005 g, Na_3 citrate 0.1 g, glucose 0.4 g, L-cysteine 0.04 g, and glycine 0.04 g. All chemicals were purchased from Sigma. Hyperoxia was obtained saturating CM with oxygen. The temperatures 25 °C and 28 °C have been selected. Indeed, the temperature range 24–30 °C has been checked to have no influence on the parameters considered in all our reported experiments.

On the space station or on a space craft, the gravitational force is approximately 10^{-4} to 10^{-6} g. There are bioreactors for cell cultures capable of modelling aspects of microgravity and the average gravitational force acting on the cells is reduced to about 10^{-2} to 10^{-3} [18–20]. However, for simplicity, we refer to these conditions of hypogravity as simulated microgravity (sim-μg). These devices are valuable to develop hypothesis concerning gravitational cell biology, to direct the design, scope, and also to substantiate orbital flight studies.

To simulate microgravity the rotating wall vessel bioreactor (RWV, Synthecon Inc, Houston, TX, USA) was used [21]. In this device, a 10-mL high aspect ratio vessel (HARV) rotates around an horizontal axis (28 rpm) and allows the gas diffusion across a semipermeable membrane. The vessel wall and the medium containing cells rotate at the same speed, producing a vector-averaged gravity comparable with that of near-earth free-fall orbit [19]. On the bases of previous studies, we calculated that the cells are exposed to reduced gravity levels of approximately 10^{-2} g [18–20]. *S. cerevisiae* was incubated in 10 mL HARV with the CM in normoxia or hyperoxia for 24 hours at 28 °C.

Cell number was determined using a Coulter Counter-Particle Count and Size Analyser, Model Z2 on mildly sonicated and diluted samples as previously described [22]. Bud scar distribution was examined by UV fluorescence microscopy after chitin staining with Calcofluor White (CW). Total protein concentration was determined using the BCATM Protein Assay Kit (Pierce). pH values were determined using a pH meter Hanna HI 221.

2.2. The SCORE experiment hardware (EH)

The SCORE EH is an automated apparatus for cell culture (CC) and fixation designed for spaceflight. It consists of a battery pack, an electronic board, a peristaltic pump, and two separated bioreactors, including two variable volume modules (VVM) each. Each VVM (20 mL) consists of two chambers separated by a sliding piston. One VVM of each bioreactor is dedicated to CC and CM, the other to fixatives. A filter inside the CC chamber allows the separation between cells and liquids. The choice of materials was done considering the peculiar requirements of the EH: resistance to vibrations, hypergravity, chemicals, and low gas permeability. Plexiglass for CC chamber and media reservoirs, Pharmed for tubes, and Teflon for the o-rings were selected. To separate the yeast and the medium at the end of the experiment, suitable filters (Millipore, 0.25 μm) were used. Hyperoxia was obtained saturating CM with oxygen. Although the selected temperature was 28 °C, the temperature recorded throughout the 24-hour spaceflight experiment was 25 ± 0.2 °C due to FOTON limitations. After landing and the return of the SCORE EH to our laboratory, filters and medium were frozen at −80 °C. SCORE experimental protocol is reported in Fig. 1b.

2.3. Actin depolymerisation

S. cerevisiae was cultivated at 1 g in 10 mL of CM added with 3 μM dihydrocytochalasin B (DHCB, Sigma) in normoxia or hyperoxia for 24 hours at 28 °C. We chose DHCB because it does not inhibit glucose uptake. Alternatively, *S. cerevisiae* was cultivated at 1 g in 10 mL of CM added with 10^{-4} M (*R*)-(+)-*trans*-4-(1-aminoethyl)-*N*-(4-pyridyl) cyclohexanecarboxamide dihydrochloride monohydrate (Y-27632, Sigma), in normoxia or hyperoxia for 24 hours at 28 °C.

2.4. Inhibition of chloride channels

To block chloride channels, *S. cerevisiae* was cultivated in hyperoxia for 24 hours at 28 °C in sim-μg or at 1 g with DHCB (as described above) in 10 mL of CM added with 10^{-5} M 5-nitro-2-(3-phenylpropyl-amino) benzoic acid (NPPB, water solution, Sigma).

2.5. Metabolites analyses

Ethanol and glycerol were identified analyzing the ^{1}H NMR spectra (Bruker AMX 500 WB spectrometer, 11.7 T) of the supernatant and their concentration were determined by integrating their relevant peaks versus a standard ($(CD_3)_2CO$) of known concentration.

Intra- and extracellular GSH concentration was determined according to the method previously described [23]. The samples were analyzed by reverse-phase HPLC (Agilent LC 1100) using a Merk Purosphere RP-18 column *endcapped* 5 μm and a spectrophotometric detector (λ = 210 nm). Solvent: 25 mM NaH_2PO_4, pH 3.5 with 1 M TPA; flow rate: 0.6 mL/min. GSH was identified using a GSH standard solution (Sigma). We validated the data analyzing the ^{1}H NMR spectra of the supernatant and by integrating GSH relevant peaks versus a standard

Fig. 1. SCORE spaceflight experiment. (a) Experimental hardware. (b) Experimental scheme: two parallel 3-step experiments were carried out after the initial preparation (START): one with oxygen saturated medium (hyperoxia, H) and the other with aerated medium (normoxia, N). L: launch; DW: dry weight; SM: selected medium; CC: cell culture; VVM: variable volume module. The temperature recorded throughout the 24-hour spaceflight experiment was 25 ± 0.2 °C. (c) Hyperoxia in space induces an enormous GSH extracellular release (GSH ER, % w/dw) as determined by HPLC. The earth gravity control (1*g* ctr, $n = 8$, $T = 25$ °C) results are shown as the mean value ± SEM; the SCORE results (single experiment) are the mean value ± SEM of eight independent measures. (d) The proteins in SCORE H were markedly carbonylated. Total proteins extracts, derivatized with DNPH, were separated by SDS–PAGE. Immunodecoration was performed using anti-DNP antibodies. (e) Hog1 was highly activated in SCORE H as evidenced by immunoblotting using an anti-phospho-p38 antibody which recognizes phospho-Hog1 (P-Hog1). (f) Slt2 was differently activated in SCORE H and N, as detected with anti-phospho-p44/42 MAP kinase antibody which recognizes phospho-Slt2 (P-Slt2). Graphs in d–f represent quantification by densitometric analysis of total carbonylated protein and phospho-protein levels normalized to the amounts of the total and of specific core proteins, respectively. Signals from at least three blots (for the uncropped image see Supplementary Information, Figs. S1c, d) were analyzed an expressed as mean value ± SEM; $^{SS}p < 0.001$ N versus H; $^{S}p \leq 0.01$ N versus H; $^{**}p < 0.001$ SCORE H versus 1*g* ctr H; $^{*}p \leq 0.01$ SCORE H versus 1*g* ctr H (Student's *t*-test). AU: arbitrary units.

(C_6D_6) of known concentration or, alternatively, using Glutathione Assay Kit (Sigma) according to the manufacturer's instructions.

2.6. Carbonylated proteins analysis

Yeast cells, separated by filtration, were washed once with phosphate buffered saline (PBS, pH 7.4) and resuspended in 10% vol./vol. glycerol, 2 mM EDTA and 1 mM protease inhibitor phenylmethanesulfonyl fluoride. Cells were broken with acid-washed glass beads in a Fast Prep FP120 (Bio101 Savant) through five cycles of 20 sec (4.5 speed setting), interspersed with cooling on ice. After centrifugation (18,000 rcf, 30 min, 4 °C), the resulting supernatant was clarified with an identical round of centrifugation and then frozen at −20 °C until used. Protein carbonyl groups were derivatized to 2,4-dinitrophenylhydrazone (DNP) by reacting with 2,4-dinitrophenylhydrazine (DNPH) according to Levine et al. [24]. Derivatized proteins were separated by SDS-PAGE electrophoresis on 8% polyacrylamide gels. Gels were blotted onto Hybond-P PVDF membranes (Amersham). DNP-derivatized proteins were detected with anti-DNP polyclonal antibody (ab6303, Abcam) diluted 1:3000 in PBS containing 5% fat milk and 0.1% Tween 20. Secondary antibodies were purchased from Amersham and diluted 1:10,000 in PBS, 5% fat milk, and 0.3% Tween 20. The binding was visualized with the ECL Western Blotting Detection Reagent (Amersham). Correct loading was confirmed by staining filters with Coomassie Brilliant Blue.

2.7. MAP kinases analysis

Cells were lysed with acid-washed glass beads in SDS Sample buffer supplemented with Phosphatase Inhibitor Cocktail 2 (Sigma) and EDTA-free Complete Protease Inhibitor Cocktail (Roche). SDS-PAGE was performed on 10% polyacrylamide gels. After blotting on nitrocellulose membrane (Protran), filters were stained for total protein with Ponceau Red (Sigma) before immunolabelling. The following primary antibodies (1:1000 diluted) were used: anti-phospho-p38 (pThr180/pTyr182) (Cell Signaling Technology) that is specific to phospho-Hog1, anti-Hog1 (y-215) (Santa Cruz Biotechnology), anti-phospho-p44/42 (Thr202/Thr204), and anti-p44/42 MAP kinase (Cell Signaling Technology). Horseradish peroxidase-conjugated anti-rabbit antibodies (Amersham) were diluted 1:10,000. Blots were developed as above.

2.8. Reverse transcription (RT)–PCR

Total RNA extraction, DNase I digestion, and RNA cleanup were performed as previously described [25]. RT-PCR was carried out to amplify the *GSH1*, *GSH2*, *GTT1*, *CTT1*, *HSP26*, *YCF1*, and *BPT1* mRNAs and 16S rRNA using the iScript cDNA Synthesis kit and iTaq DNA Polymerase (Bio-Rad) according to the manufacturer's instructions. The number of cycles was lowered to 15/20 so that amplification was in the

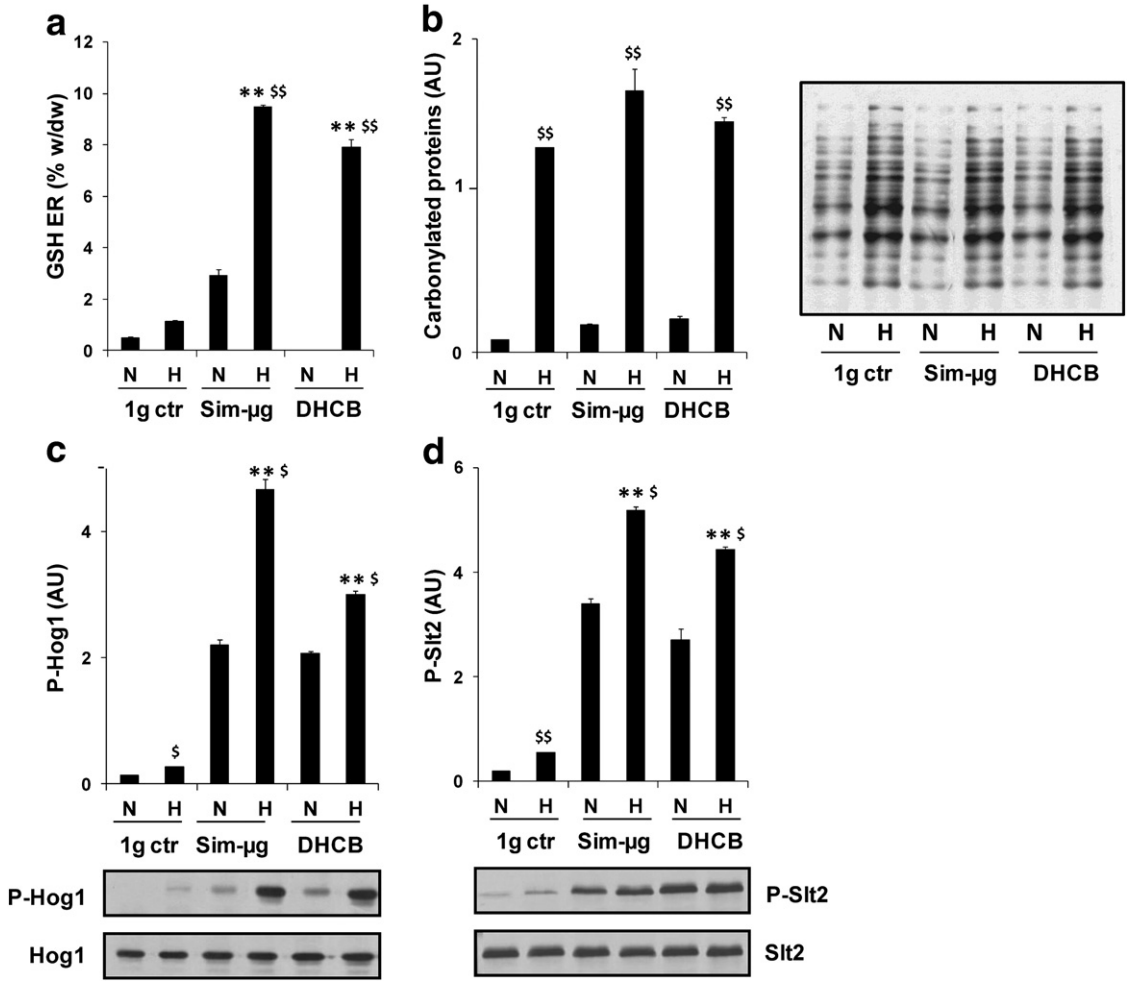

Fig. 2. Replication of the spaceflight experiments under conditions of simulated microgravity (sim-µg), and at 1 g using dihydrocytochalasin B (DHCB). Microgravity was simulated using the rotating wall vessel bioreactor (RWV, Synthecon). (a) A significantly high GSH ER (% w/dw) was observed in sim-µg H and DHCB H, compared to the related 1g ctr H. Results are shown as the mean value ± SEM ($n = 20$). (b) The proteins were carbonylated to similar extent under all of the hyperoxic conditions. Hog1 (c) and Slt2 (d) were activated in both sim-µg and DHCB. See Fig. 1 for the abbreviations and technical details. Signal intensities reported in graphs b–d were analyzed from at least three blots (for uncropped images see Supplementary Information, Fig. S2) and expressed as mean value ± SEM; $^{\$\$}p < 0.001$ N versus H; $^{\$}p \leq 0.01$ N versus H; $^{**}p < 0.001$ sim-µg H or DHCB H versus 1g ctr H; $^{*}p \leq 0.01$ sim-µg H or DHCB H versus 1g ctr H (Student's *t*-test).

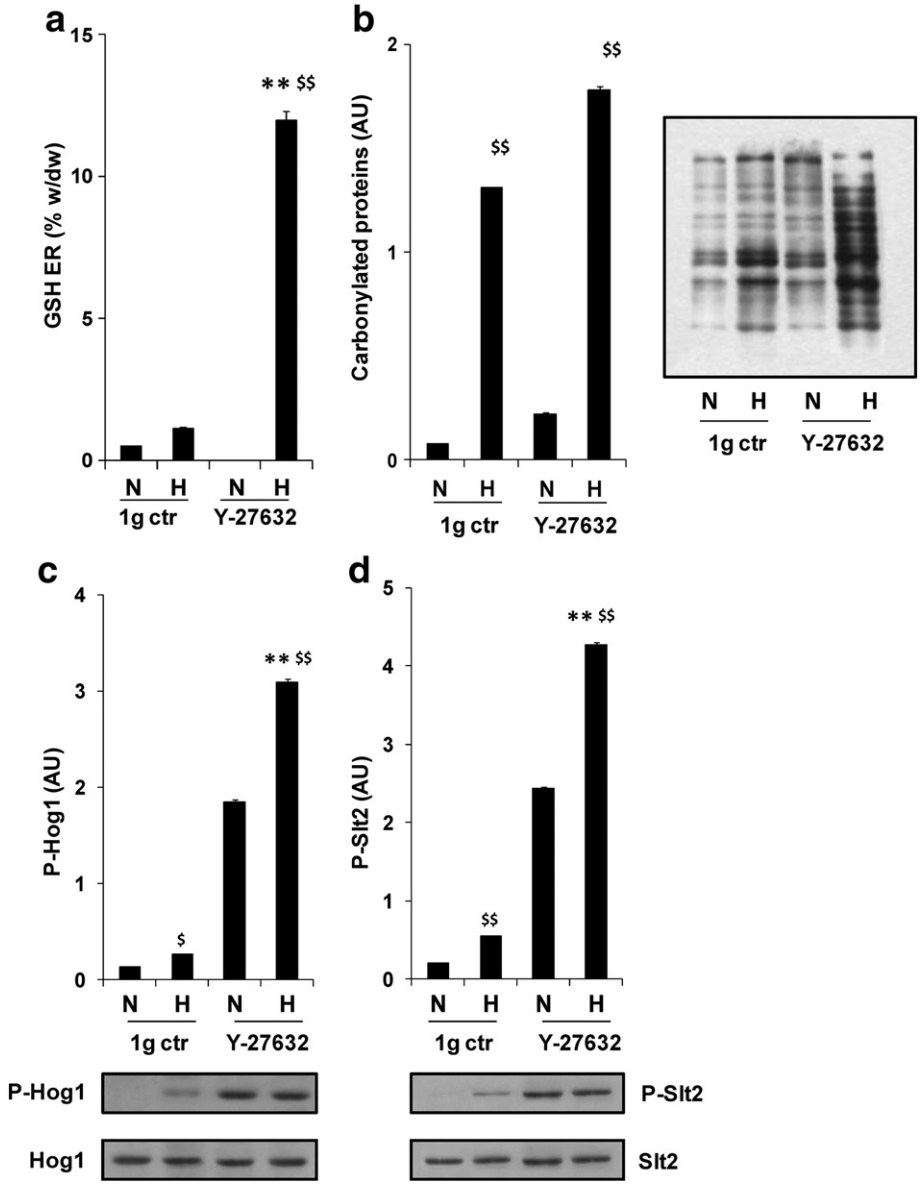

Fig. 3. Replication of the spaceflight experiments at 1 g using (*R*)-(+)-*trans*-4-(1-aminoethyl)-*N*-(4-pyridyl)cyclohexanecarboxamide dihydrochloride monohydrate (Y-27632). (a) A significantly high GSH ER (% w/dw) was observed in Y-27632 H, compared to the related 1*g* ctr H. The results are the mean value ± SEM ($n = 8$). (b) The proteins were carbonylated to similar extent under hyperoxic conditions. Hog1 (c) and Slt2 (d) were activated during the Y-27632 treatment. See Fig. 1 for the abbreviations and technical details. Signal intensities reported in graphs b–d were analyzed from at least three blots (for uncropped images see Supplementary Information, Fig. S3) and were expressed as mean value ± SEM; $^{\$\$}p < 0.001$ N versus H; $^{\$}p \leq 0.01$ N versus H; $^{**}p < 0.001$ Y-27632 H versus 1*g* ctr H; $^{*}p \leq 0.01$ Y-27632 H versus 1*g* ctr H (Student's *t*-test).

exponential range. Quantification was performed by using Image J software. Intensity values were normalized according to the 16S rRNA level. Experiments were repeated at least twice with different RNA preparations. Primer sequences are available upon request.

2.9. Statistical analysis

Student's *t* test was used to determine statistical significance. Results are expressed as the mean ± SEM from an appropriate number of experiments as indicated in the figure legends. $P \leq 0.01$ was considered statistically significant.

3. Results and discussion

3.1. The SCORE spaceflight experiment

The FOTON-M3 space mission allowed us to investigate the oxidative stress response of *S. cerevisiae* under conditions of real microgravity. SCORE involved two parallel experiments designed to distinguish the effects of oxidative stress and microgravity: one under hyperoxic conditions (oxygen, SCORE hyperoxia) and one under normoxic conditions (air, SCORE normoxia). Fig. 1 shows the cultivation system (Fig. 1a) developed in collaboration with Thales Alenia Space, the experimental

Fig. 4. Twenty-four-hour profiles of intra- and extracellular GSH, ethanol and glycerol concentrations, and pH in 1*g* ctr, sim-μg, and DHCB under hyperoxic conditions. The cells were harvested and their intra- and extracellular GSH (% w/dw), and ethanol and glycerol concentrations, and pH were determined at selected time points. (a, a′) In the 1*g* ctr experiment, GSH ER is very low, while ethanol and glycerol releases are as expected. (b) In sim-μg GSH ER occurred between 10 and 11 hours after $t = 0$ and, at the same time, intracellular GSH peaked, and then returned to its initial level. (c) The addition of 5-nitro-2-(3-phenylpropyl-amino) benzoic acid (NPPB), completely blocked GSH ER, while pH value remains in the range 4.8–5.4. (d) Similarly, but 4 hours earlier, the presence of DHCB under hyperoxic conditions, caused GSH ER in 1 hour. (e) The addition of NPPB completely blocked GSH ER while pH value remains in the range 4.8–5.4. (b′-e′) Twenty-four-hour profiles of ethanol and glycerol releases in all the reported conditions.

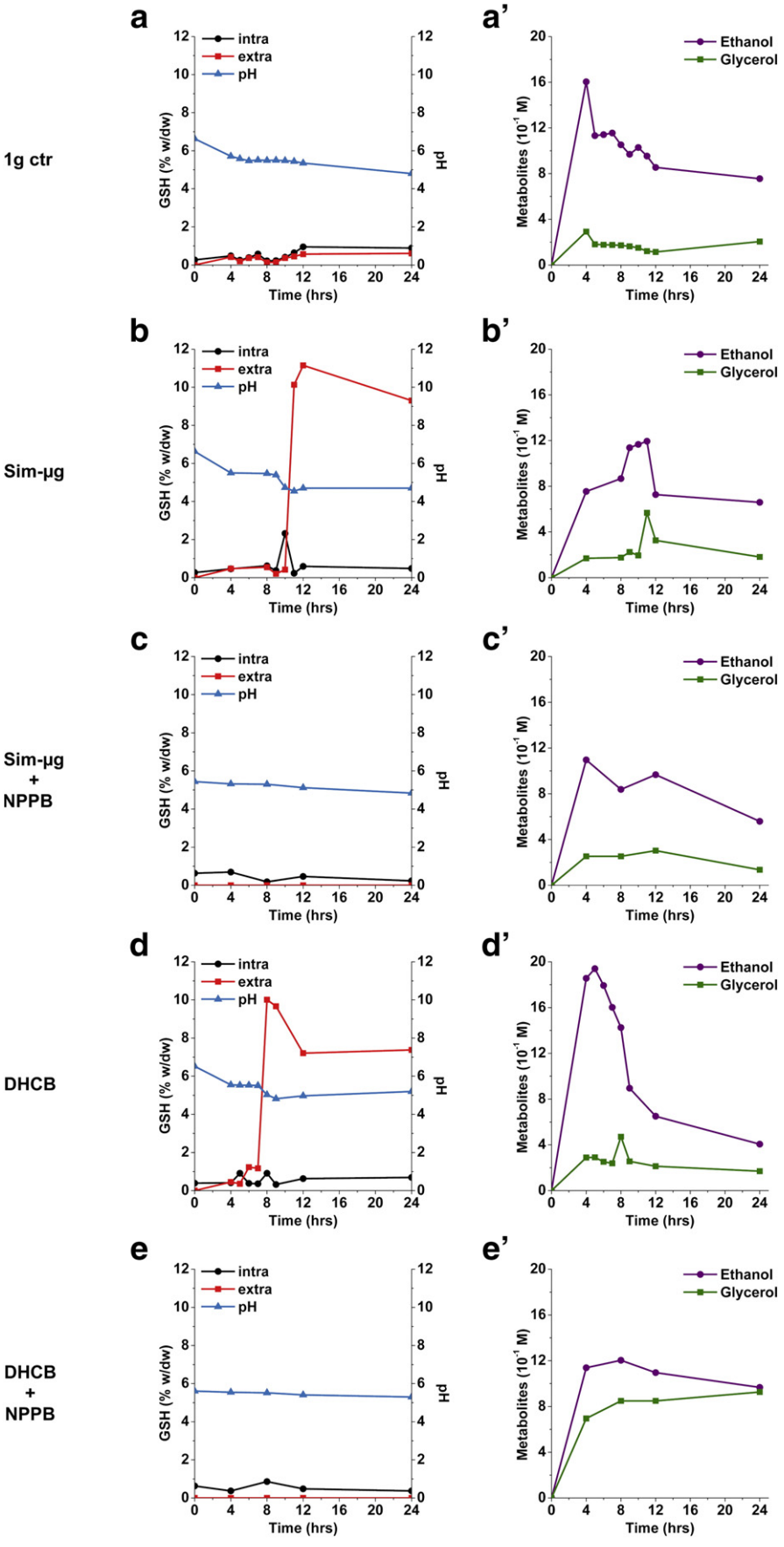
a
a'
1g ctr
b
b'
Sim-µg
c
c'
Sim-µg
+
NPPB
d
d'
DHCB
e
e'
DHCB
+
NPPB
intra
extra
pH
GSH (% w/dw)
pH
Time (hrs)
Ethanol
Glycerol
Metabolites (10⁻¹ M)

protocol (Fig. 1b) and results (Figs. 1c–f). As spaceflight constraints limited the choice of fixatives for the ground analyses of the flown samples, we concentrated on GSH and cell wall stress responses rather than actin cytoskeleton imaging because it is well known that various cell types cultured in microgravity undergo cytoskeletal rearrangements [26–28].

SCORE was completely successful in both engineering and biochemical terms. We confirmed that the yeast cells were metabolically active during the spaceflight experiment as they completely consumed extracellular glucose, produced ethanol and glycerol as expected (Supplementary information, Figs. S1a, b), and maintained a high intracellular trehalose content (data not shown) in response to the imposed stress. We also found that our hyperoxic conditions had oxidative consequences because there was a marked increase in protein carbonylation (Fig. 1d), one of the principal and most frequently observed oxidative alterations [29].

Analysis of the spaceflight samples (Figs. 1c–f) showed that 24 hours of hyperoxia induced an enormous GSH ER (≈40% w/dw), thus validating our hypothesis that microgravity plays a major role. In addition, the yeast responded to the imposed stress by activating two major pathways: high-osmolarity glycerol (HOG) MAP kinase and cell integrity/protein kinase C (PKC) pathways. HOG monitors cell swelling or shrinking and senses oxidative stress, whereas PKC responds to changes in cell morphology by controlling the expression of genes involved in the cell wall biogenesis and the reorganisation of the actin cytoskeleton [30]. In detail, we considered the two proteins Hog1 and Slt2. Hog1 was highly activated only under the SCORE hyperoxic conditions (as a result of the combined effects of microgravity and oxidative stress), whereas Slt2, which senses the microgravity environment, was activated under both SCORE hyperoxic and SCORE normoxic conditions. In line with previous space mission results [27], there was a two-fold increase in random budding, although the budding frequency was very low (≈20%), due to our culture conditions.

The SCORE results were due to various conditions acting together: 1) fermentation in an essential medium optimised for GSH production, 2) microgravity, and 3) oxidative stress. They can find a logical interpretation. Briefly, hyperoxia and the optimised medium stimulate intracellular GSH production. Microgravity induces responses that are similar to those generated by an osmotic shock [16] capable of mediating cytoskeletal rearrangements, and this activates the yeast's volume-sensitive ion channels through which GSH is released.

3.2. Ground experiments

3.2.1. Spaceflight simulation

To validate the results of the single space experiment, we performed a complete set of sim-μg experiments under hyperoxic and normoxic conditions, using the RWV bioreactor. We are confident of the reliability of our results because we had previous experience with various simulators [31–33] confirming data obtained in real microgravity [34], thus suggesting the suitability of using these surrogate systems for bench-top microgravity research.

These experiments (Figs. 2a-d) give significance to our spaceflight results because of the clear evidence of a high rate of GSH ER (≈10% w/dw) with protein carbonylation under hyperoxic conditions, Hog1 and Slt2 activation under both normoxic and hyperoxic conditions, and a 1.7-fold increase in random budding. The fact that some of the sim-μg values are lower than those obtained in the spaceflight experiment is due to the limitations of the sim-μg device.

In addition, there were no changes in cell viability in comparison with the related ground controls, as confirmed by the evaluation of the number of colony-forming units (CFUs). Furthermore, high-osmolarity, sodium dodecyl sulphate, and calcofluor white plate-sensitivity assays indicated no major changes in cell wall integrity or permeability (data not shown).

The increase in random budding and the activation of the cell integrity pathway observed in the space and sim-μg experiments indicated that the observed effects are mainly due to cytoskeletal alterations [30].

3.2.2. Chemical cytoskeletal modifications at 1 g confirm actin involvement in the extracellular release of GSH in hyperoxia

To determine whether the high rate of GSH ER was the yeast's response to microgravity-mediated cytoskeletal alterations, we treated cells on ground with dihydrocytochalasin B (DHCB), a well known inhibitor of actin polymerisation [35], under normoxic and hyperoxic conditions using the same analytical protocol. As in the case of the sim-μg and SCORE experiments, the results (Figs. 2a–d) indicated a high rate of GSH ER (≈8% w/dw) with protein carbonylation under hyperoxic conditions, Hog1 and Slt2 activation, and a 1.5-fold increase in random budding. Furthermore, no changes in cell viability or in cell wall integrity or permeability, in comparison with the related ground controls, were detected (data not shown).

These data were confirmed by treating cells on ground with (*R*)-(+)-*trans*-4-(1-aminoethyl)-*N*-(4-pyridyl)cyclohexanecarboxamide dihydrochloride monohydrate (Y-27632), a potent and selective ROCK inhibitor [36], under normoxic and hyperoxic conditions because it has been shown that the ROCK family of kinases is involved in the Rho-induced, myosin-dependent contraction and formation of actin stress fibres. As shown in Figs. 3a–d, and as in the case of the SCORE, sim-μg, and DHCB experiments, Y-27632 induced a high rate of GSH ER (≈12% w/dw) with protein carbonylation under hyperoxic conditions, Hog1 and Slt2 activation, and a 1.6-fold increase in random budding.

3.2.3. The dynamics of the GSH ER together with the evaluation of the expression of selected genes

We wanted to discriminate whether GSH is released throughout the 24 hours' experiment or in a certain time range. Fig. 4 shows the dynamics of the GSH ER due to hyperoxia in sim-μg and after DHCB treatment. In sim-μg (Figs. 4b–b′) GSH ER occurred between 10 and 11 hours after the start of fermentation ($t=0$); at the same time, intracellular GSH peaked (≈2.3% w/dw) and then shortly returned to its initial level (≈0.5% w/dw). Similarly, but 4 hours earlier, the presence of DHCB under hyperoxic conditions (Figs. 4d–d′) induced GSH ER in 1 hour, but intracellular GSH appeared to be less modulated. Under both experimental conditions, glycerol concentrations increased in 1 hour at the same time as GSH ER. The results of the 1 *g* control experiment under hyperoxic conditions were as expected (Figs. 4a–a′).

As *S. cerevisiae* gene expression has been extensively studied under conditions of oxidative stress [12] and sim-μg [15–17], we analysed the transcript levels of selected genes to determine whether the GSH ER observed under our experimental conditions can be associated with a mechanism of transcriptional regulation. In particular, we considered *GSH1* and *GSH2*, encoding a gamma glutamylcysteine synthetase and a glutathione sinthetase respectively, that catalyse the two main steps of GSH biosynthesis; *GTT1*, encoding GSH transferase 1; *BPT1* and *YCF1*, encoding two vacuolar GSH *S*-conjugate transporters of the ATP-binding cassette family; and two genes involved in stress response: heat shock protein 26 (*HSP26*) and *CTT1*, encoding the cytosolic catalase T. Their mRNA levels were analysed at selected time points in sim-μg, DHCB and 1*g* ctr cells (Fig. 5). High levels of *HSP26* and *CTT1* transcripts were observed between 4 and 9 hours in the sim-μg samples and they were still detectable after 11–12 hours. Very similar behaviour was observed in the samples treated with DHCB, whereas neither of the mRNAs was observed in the 1*g* ctr cells. The transcription of these genes indicates that cells activated a transcriptional response mediated by the MAP kinases pathway [37], which is in line with the observed activation of Hog1. Furthermore, active *CTT1* transcription indicated the activation of a specific defence against oxidative stress.

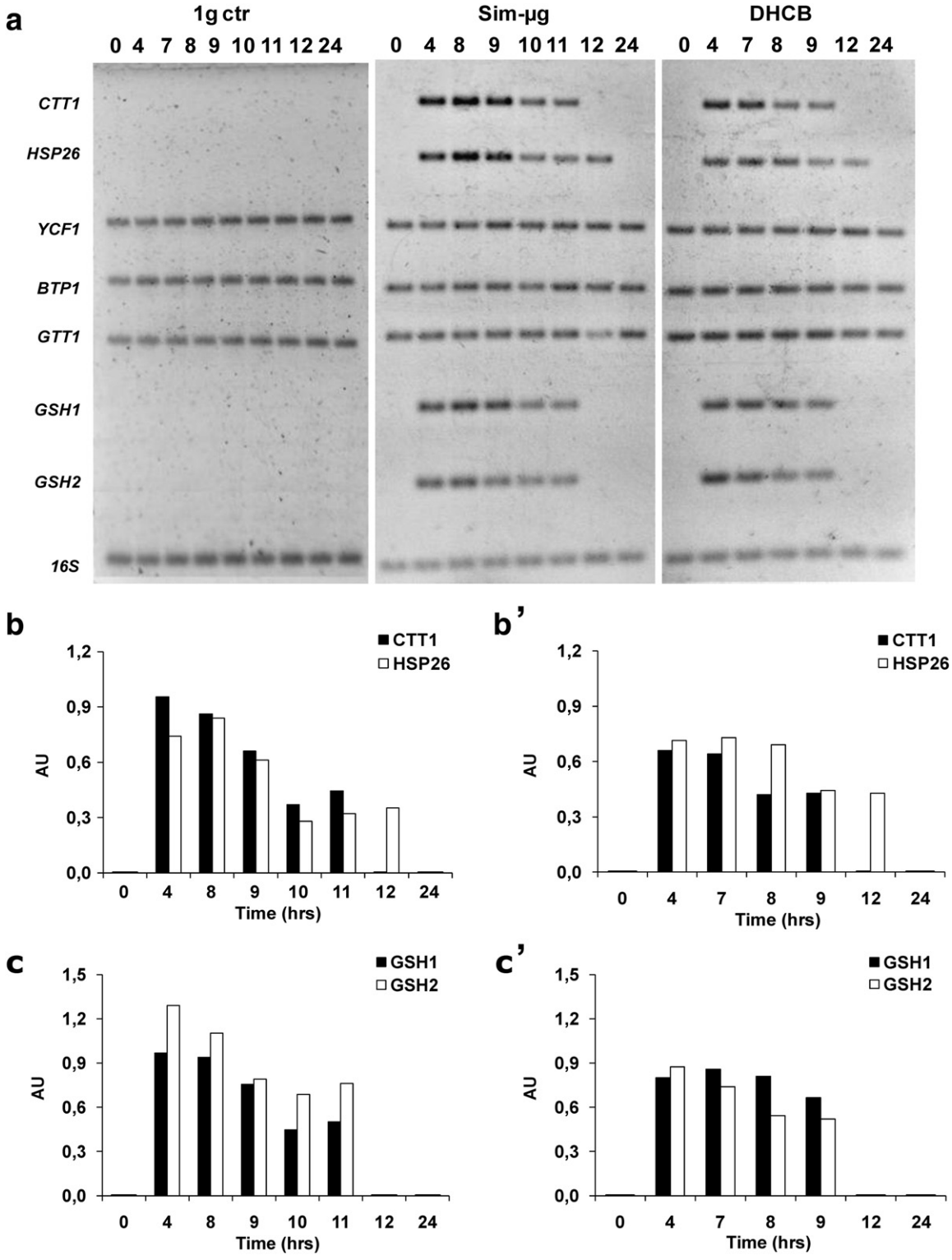

Fig. 5. Twenty-four-hour gene expression profiles in 1*g* ctr, sim-µg, and DHCB under hyperoxic conditions. (a) At selected time points, the cells were harvested and a semiquantitative RT–PCR was carried out to amplify *GSH1*, *GSH2*, *GTT1*, *CTT1*, *HSP26*, *YCF1*, and *BPT1* mRNAs and 16S rRNA (used as control). In sim-µg, *GSH1*, *GSH2*, *HSP26*, and *CTT1* were upregulated: highly expressed between 4 and 11 hours, and peaking between 8 and 9 hours. A similar trend was observed in DHCB, although high expression levels were reached between 4 and 9 hours, and peak levels between 7 and 8 hours. Differently, *GTT1*, *BPT1*, and *YCF1* mRNAs were present from the start of the experiment under all conditions, indicating that these genes were expressed but did not undergo any transcriptional modulation. Changes of the transcript levels were estimated as relative abundance and calculated by densitometric analysis. Intensity values were normalized according to the 16S rRNA level. (b, c) Sim-µg. (b′, c′) DHCB.

GSH1 and *GSH2* transcripts appeared in the sim-µg and DHCB cells after 4 hours, and were detectable until GSH ER stopped. On the contrary *GTT1, BPT1* and *YCF1* mRNAs were present from the start of the experiment under all conditions, which indicates that these genes were expressed but did not undergo transcriptional modulation; it therefore seems that they are unrelated to the observed GSH ER. The comparable abundance of *YCF1* and *BPT1* transcripts is in line with published observations [38]; in particular, a high level of *BPT1* mRNA is

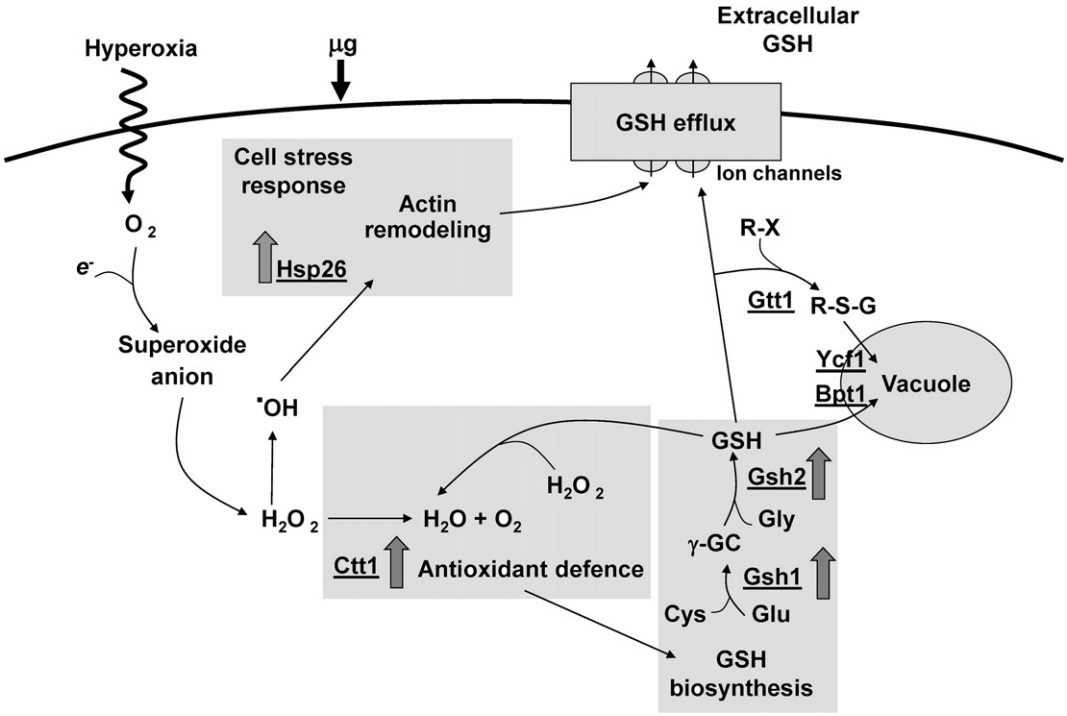

Fig. 6. Schematic model of the combined effects of microgravity (μg) and hyperoxia on GSH efflux. In yeast, GSH synthesis requires two sequential reactions catalyzed by Gsh1 and Gsh2. The former synthesizes L-γ-glutamylcysteine (γ-GC), from L-cysteine (Cys) and L-glutamate (Glu), the latter adds a glycine (Gly) to γ-GC. Moreover, the level of free reduced GSH depends on the balance between biosynthesis and conjugation. In particular, the GSH *S*-transferase Gtt1 uses GSH as an acceptor of electrophilic substrates (*R*-X) to form glutathione conjugates (R-S-G). H_2O_2 can be detoxified by GSH-dependent activities and by the cytoplasmic catalase Ctt1 that reduces H_2O_2 to water. In parallel with such scavenging enzymatic defences, the cellular stress response also involves Hsp26. In the GSH transport to the vacuole, the yeast cadmium factor-1, Ycf1, and the bile pigment transporter-1, Bpt1, are required. The gene products of some selected genes analyzed in this work are underlined. Similar combined effects can be depicted for DHCB treatment under hyperoxic conditions. See the text for more details.

consistent with the high levels of Bpt1 in the early stationary phase due to its function in vacuolar detoxification [39]. These results indicate that sim-μg or DHCB under hyperoxic conditions affect the transcription of the genes involved in GSH biosynthesis and stress response but not in vacuolar transport (Fig. 6).

3.2.4. Involvement of the chloride channels in the GSH ER

Although their final effects are very similar, microgravity (real and simulated), DHCB and Y-27632 act differently. DHCB and Y-27632 depolymerise actin fibers, whereas microgravity alters the organisation of cytoskeleton machinery. In all of the considered cases, cells respond to the imposed stresses by activating volume-sensitive ion channels [40–44].

Working on the hypothesis that anionic GSH is permeant in chloride channels, as observed in cystic fibrosis [45], we repeated the sim-μg and DHCB experiments under hyperoxic conditions by adding the potent chloride channel blocker [42] 5-nitro-2-(3-phenylpropylamino) benzoic acid (NPPB) to the culture medium. In both cases, NPPB completely blocked GSH ER (Figs. 4c, c′, e, and e′), thus confirming the key involvement of chloride channels (Fig. 6).

4. Conclusions

SCORE took advantage of the extreme space environment to investigate the mechanisms responsible for GSH loss under oxidative conditions.

We are aware that the experiment has a number of limitations due to the well-known inconveniences of space biology, including the strictly limited number of samples and possible fixatives. Furthermore, the yeast cells were grown in an essential medium (i.e., under conditions close to stationary phase) that only contained a carbon source, some salts and the amino acids required to produce GSH, and we used mild oxidative stress to avoid the extensive chemical deterioration of our system.

Nevertheless, all of the experiments demonstrate that: 1) gravitational unloading induces the disorganisation of actin, and this causes critical cytoskeleton rearrangements that determine the activation of the volume-sensitive ion channels though which GSH is released; 2) the induction of actin alterations by means of two chemical compounds (DHCB and Y-27632) causes similar GSH ER in the presence of oxidative stress; and 3) in all cases, the actin-related activation of chloride channels is the main process responsible for GSH ER.

We are confident that these results significantly contribute to a better understanding of the mechanisms affecting GSH homeostasis in higher eukaryotes, and may provide insights into the underlying cause of GSH depletion in many diseases.

The following are the supplementary materials related to this article. Supplementary materials related to this article can be found online at 10.1016/j.bbamcr.2010.07.007.

Acknowledgments

The study was supported by the Italian Space Agency (ASI: contract no. 1-006/06/1 “DCMC” 1B1118, coordinator: S. Bradamante). We would like to thank dr. ing. M. Freddi and G. Falcetti of Thales Alenia Space for the design, development, and support in the preparation of the SCORE experimental hardware and I. Sagot of the Institut de Biochimie et Génétique Cellulaire CNRS, Bordeaux, France, for her technical advice, assistance and critical discussions.

References

[1] E. Wang, Age-dependent atrophy and microgravity travel: what do they have in common? FASEB J. 13 (Suppl) (1999) S167–S174.
[2] G. Biolo, M. Heer, M. Narici, F. Strollo, Microgravity as a model of ageing, Curr. Opin. Clin. Nutr. Metab. Care 6 (2003) 31–40.

[3] H.L. Nichols, N. Zhang, X. Wen, Proteomics and genomics of microgravity, Physiol. Genomics 26 (2006) 163–171.
[4] T.P. Stein, M.J. Leskiw, Oxidant damage during and after spaceflight, Am. J. Physiol. Endocrinol. Metab. 278 (2000) E375–E382.
[5] D.P. Jones, Radical-free biology of oxidative stress, Am. J. Physiol. Cell Physiol. 295 (2008) C849–C868.
[6] J. Hollander, M. Gore, R. Fiebig, R. Mazzeo, S. Ohishi, H. Ohno, L.L. Ji, Spaceflight downregulates antioxidant defense systems in rat liver, Free Radic. Biol. Med. 24 (1998) 385–390.
[7] N. Ballatori, S.M. Krance, S. Notenboom, S. Shi, K. Tieu, C.L. Hammond, Glutathione dysregulation and the etiology and progression of human diseases, Biol. Chem. 390 (2009) 191–214.
[8] S. Bradamante, L. Barenghi, A. Villa, A bioreactor, in particular for NMR spectroscopy. Patent US 7695957 B2 (2010).
[9] S. Versari, A. Villa, L. Barenghi, S. Bradamante, Advantages of simulated microgravity in the production of compounds of industrial relevance, European Space Agency SP-585 (2005) versari/1–versari/2 [Special Publication].
[10] A.H. Tong, G. Lesage, G.D. Bader, H. Ding, H. Xu, X. Xin, J. Young, G.F. Berriz, R.L. Brost, M. Chang, Y. Chen, X. Cheng, G. Chua, H. Friesen, D.S. Goldberg, J. Haynes, C. Humphries, G. He, S. Hussein, L. Ke, N. Krogan, Z. Li, J.N. Levinson, H. Lu, P. Menard, C. Munyana, A.B. Parsons, O. Ryan, R. Tonikian, T. Roberts, A.M. Sdicu, J. Shapiro, B. Sheikh, B. Suter, S.L. Wong, L.V. Zhang, H. Zhu, C.G. Burd, S. Munro, C. Sander, J. Rine, J. Greenblatt, M. Peter, A. Bretscher, G. Bell, F.P. Roth, G.W. Brown, B. Andrews, H. Bussey, C. Boone, Global mapping of the yeast genetic interaction network, Science 303 (2004) 808–813.
[11] A.P. Gasch, P.T. Spellman, C.M. Kao, O. Carmel-Harel, M.B. Eisen, G. Storz, D. Botstein, P.O. Brown, Genomic expression programs in the response of yeast cells to environmental changes, Mol. Biol. Cell 11 (2000) 4241–4257.
[12] M.D. Temple, G.G. Perrone, I.W. Dawes, Complex cellular responses to reactive oxygen species, Trends Cell Biol. 15 (2005) 319–326.
[13] G.W. Thorpe, C.S. Fong, N. Alic, V.J. Higgins, I.W. Dawes, Cells have distinct mechanisms to maintain protection against different reactive oxygen species: oxidative-stress-response genes, Proc. Natl. Acad. Sci. U. S. A. 101 (2004) 6564–6569.
[14] C.E. Outten, R.L. Falk, V.C. Culotta, Cellular factors required for protection from hyperoxia toxicity in *Saccharomyces cerevisiae*, Biochem. J. 388 (2005) 93–101.
[15] K. Johanson, P.L. Allen, R.A. Gonzalez-Villalobos, C.B. Baker, R. D'Elia, T.G. Hammond, Gene expression and survival changes in *Saccharomyces cerevisiae* during suspension culture, Biotechnol. Bioeng. 93 (2006) 1050–1059.
[16] C.A. Nickerson, C.M. Ott, J.W. Wilson, R. Ramamurthy, D.L. Pierson, Microbial responses to microgravity and other low-shear environments, Microbiol. Mol. Biol. Rev. 68 (2004) 345–361.
[17] B. Purevdorj-Gage, K.B. Sheehan, L.E. Hyman, Effects of low-shear modeled microgravity on cell function, gene expression, and phenotype in *Saccharomyces cerevisiae*, Appl. Environ. Microb. 72 (2006) 4569–4575.
[18] N. Rucci, A. Rufo, M. Alamanou, A. Teti, Modeled microgravity stimulates osteoclastogenesis and bone resorption by increasing osteoblast RANKL/OPG ratio, J. Cell. Biochem. 100 (2007) 464–473.
[19] B.R. Unsworth, P.I. Lelkes, Growing tissues in microgravity, Nat. Med. 4 (1998) 901–907.
[20] D.F. Meaney, E.D. Johnston, M. Litt, S.R. Pollack, Experimental and numerical investigations of microcarrier motions in simulated microgravity, Adv. Heat Mass Transf. Biotechnol. HTD 362 (1998) 103–107.
[21] T.G. Hammond, J.M. Hammond, Optimized suspension culture: the rotating-wall vessel, Am. J. Physiol. Renal Physiol. 281 (2001) F12–F25.
[22] M. Vanoni, M. Vai, L. Popolo, L. Alberghina, Structural heterogeneity in populations of the budding yeast *Saccharomyces cerevisiae*, J. Bacteriol. 156 (1983) 1282–1291.
[23] J. Lakritz, C.G. Plopper, A.R. Buckpitt, Validated high-performance liquid chromatography–electrochemical method for determination of glutathione and glutathione disulfide in small tissue samples, Anal. Biochem. 247 (1997) 63–68.
[24] R.L. Levine, J.A. Williams, E.R. Stadtman, E. Shacter, Carbonyl assays for determination of oxidatively modified proteins, Method. Enzymol. 233 (1994) 346–357.
[25] I. Orlandi, M. Bettiga, L. Alberghina, M. Vai, Transcriptional profiling of ubp10 null mutant reveals altered subtelomeric gene expression and insurgence of oxidative stress response, J. Biol. Chem. 279 (2004) 6414–6425.
[26] M.L. Lewis, J.L. Reynolds, L.A. Cubano, J.P. Hatton, B.D. Lawless, E.H. Piepmeier, Spaceflight alters microtubules and increases apoptosis in human lymphocytes (Jurkat), FASEB J. 12 (1998) 1007–1018.
[27] I. Walther, B. Bechler, O. Muller, E. Hunzinger, A. Cogoli, Cultivation of *Saccharomyces cerevisiae* in a bioreactor in microgravity, J. Biotechnol. 47 (1996) 113–127.
[28] M. Hughes-Fulford, M.L. Lewis, Effects of microgravity on osteoblast growth activation, Exp. Cell Res. 224 (1996) 103–109.
[29] I. Dalle-Donne, D. Giustarini, R. Colombo, R. Rossi, A. Milzani, Protein carbonylation in human diseases, Trends Mol. Med. 9 (2003) 169–176.
[30] S. Hohmann, Osmotic stress signaling and osmoadaptation in yeasts, Microbiol. Mol. Biol. Rev. 66 (2002) 300–372.
[31] S. Versari, A. Villa, S. Bradamante, J.A.M. Maier, Alterations of the actin cytoskeleton and increased nitric oxide synthesis are common features in human primary endothelial cell response to changes in gravity, Biochim. Biophys. Acta 7 (2007) 7.
[32] A. Villa, S. Versari, L. Barenghi, J.A.M. Maier, S. Bradamante, Effects of spaceflight simulation on human cells, European Space Agency SP SP-585 (2005) villa/1–villa/2 [Special Publication].
[33] A. Villa, S. Versari, J.A. Maier, S. Bradamante, Cell behavior in simulated microgravity: a comparison of results obtained with RWV and RPM, Gravit. Space Biol. Bull. 18 (2005) 89–90.
[34] J.P. Hatton, F. Gaubert, M.L. Lewis, Y. Darsel, P. Ohlmann, J.P. Cazenave, D. Schmitt, The kinetics of translocation and cellular quantity of protein kinase C in human leukocytes are modified during spaceflight, FASEB J. 13 (Suppl) (1999) S23–S33.
[35] J.A. Cooper, Effects of cytochalasin and phalloidin on actin, J. Cell Biol. 105 (1987) 1473–1478.
[36] T. Ishizaki, M. Uehata, I. Tamechika, J. Keel, K. Nonomura, M. Maekawa, S. Narumiya, Pharmacological properties of Y-27632, a specific inhibitor of rho-associated kinases, Mol. Pharmacol. 57 (2000) 976–983.
[37] C. Schuller, J.L. Brewster, M.R. Alexander, M.C. Gustin, H. Ruis, The HOG pathway controls osmotic regulation of transcription via the stress response element (STRE) of the *Saccharomyces cerevisiae CTT1* gene, EMBO J. 13 (1994) 4382–4389.
[38] K.G. Sharma, D.L. Mason, G. Liu, P.A. Rea, A.K. Bachhawat, S. Michaelis, Localization, regulation, and substrate transport properties of Bpt1p, a *Saccharomyces cerevisiae* MRP-type ABC transporter, Eukaryot. Cell 1 (2002) 391–400.
[39] M. Klein, Y.M. Mamnun, T. Eggmann, C. Schuller, H. Wolfger, E. Martinoia, K. Kuchler, The ATP-binding cassette (ABC) transporter Bpt1p mediates vacuolar sequestration of glutathione conjugates in yeast, FEBS Lett. 520 (2002) 63–67.
[40] N. Ahmed, M. Ramjeesingh, S. Wong, A. Varga, E. Garami, C.E. Bear, Chloride channel activity of ClC-2 is modified by the actin cytoskeleton, Biochem. J. 352 (Pt 3) (2000) 789–794.
[41] K. Flis, P. Bednarczyk, R. Hordejuk, A. Szewczyk, V. Berest, K. Dolowy, A. Edelman, A. Kurlandzka, The Gef1 protein of *Saccharomyces cerevisiae* is associated with chloride channel activity, Biochem. Biophys. Res. Commun. 294 (2002) 1144–1150.
[42] A. Lopez-Rodriguez, A.C. Trejo, L. Coyne, R.F. Halliwell, R. Miledi, A. Martinez-Torres, The product of the gene GEF1 of *Saccharomyces cerevisiae* transports Cl^- across the plasma membrane, FEMS Yeast Res. 7 (2007) 1218–1229.
[43] H.F. Cantiello, Role of the actin cytoskeleton in the regulation of the cystic fibrosis transmembrane conductance regulator, Exp. Physiol. 81 (1996) 505–514.
[44] D.M. Wolfe, D.A. Pearce, Channeling studies in yeast: yeast as a model for channelopathies? Neuromol. Med. 8 (2006) 279–306.
[45] P. Linsdell, J.W. Hanrahan, Glutathione permeability of CFTR, Am. J. Physiol. 275 (1998) C323–C326.